# Quantification of Protein Hydration, Glass Transitions, and Structural Relaxations of Aqueous Protein and Carbohydrate–Protein Systems

**ARTICLE** *in* THE JOURNAL OF PHYSICAL CHEMISTRY B · MAY 2015

Impact Factor: 3.3 · DOI: 10.1021/acs.jpcb.5b01593 · Source: PubMed



**2 AUTHORS:**

Yrjö H. Roos

University College Cork

**199** PUBLICATIONS **5,785** CITATIONS

SEE PROFILE

Naritchaya Potes

University College Cork

**17** PUBLICATIONS **22** CITATIONS

SEE PROFILE

THE JOURNAL OF PHYSICAL CHEMISTRY B

Article

pubs.acs.org/JPCB

# Quantification of Protein Hydration, Glass Transitions, and Structural Relaxations of Aqueous Protein and Carbohydrate−Protein Systems

Yrjö H. Roos* and Naritchaya Potes

School of Food and Nutritional Sciences, University College Cork, Cork, Ireland

**ABSTRACT:** Water distribution and miscibility of carbohydrate and protein components in biological materials and their structural contributions in concentrated solids are poorly understood. In the present study, structural relaxations and a glass transition of protein hydration water and antiplasticization of the hydration water at low temperatures were measured using dynamic mechanical analysis (DMA) and differential scanning calorimetry (DSC) for bovine whey protein (BWP), aqueous glucose−fructose (GF), and their mixture. Thermal transitions of $\alpha$-lactalbumin and $\beta$-lactoglobulin components of BWP included water-content-dependent endothermic but reversible dehydration and denaturation, and exothermic and irreversible aggregation. An $\alpha$-relaxation assigned to hydration water in BWP appeared at water-content-dependent temperatures and increased to over the range of 150−200 K at decreasing water content and in the presence of GF. Two separate glass transitions and individual fractions of unfrozen water of ternary GF−BWP−water systems contributed to uncoupled $\alpha$-relaxations, suggesting different roles of protein hydration water and carbohydrate vitrification in concentrated solids during freezing and dehydration. Hydration water in the BWP fraction of GF−BWP systems was derived from equilibrium water sorption and glass transition data of the GF fraction, which gave a significant universal method to quantify (i) protein hydration water and (ii) the unfrozen water in protein−carbohydrate systems for such applications as cryopreservation, freezing, lyophilization, and dehydration of biological materials. A ternary supplemented phase diagram (state diagram) established for the GF−BWP−water system can be used for the analysis of the water distribution across carbohydrate and protein components in such applications.

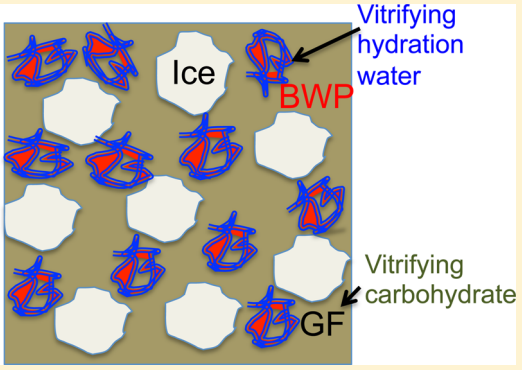


## INTRODUCTION

Protection of protein conformation and retention of biological functions subsequent to freezing and thawing or freeze-drying and rehydration have been the subject of numerous studies.[1−3] Such information is increasingly important for the understanding of the stability of bioactive pharmaceutical and food components, for example, bioactive peptides and proteins, as well as protection of cells and probiotic bacteria. The use of carbohydrates, particularly monosaccharides and disaccharides, to protect protein structures against freezing and dehydration damage has been of particular interest. The phase behavior of water and the state of dissolved substances were found to dominate thermal properties of cryoprotectant carbohydrate systems, and ice formation is known to result in separation of a freeze-concentrated unfrozen aqueous solids phase and vitrification of the maximally freeze-concentrated unfrozen phase over a carbohydrate-specific temperature range.[4−7] The phase and state behavior of binary carbohydrate−water systems may be described using state diagrams that for small sugars show miscibility and strong plasticization by water.[8,9] Such state diagrams have clarified the physicochemical properties, including the glass transition, ice formation, and ice melting properties of aqueous carbohydrate systems at low temperatures, but they lack information required for the understanding of carbohydrate−protein interactions in biological, food, and pharmaceutical systems. Conversely, the glass transition data shown in state diagrams can be used to derive water contents from measured glass transition temperatures, $T_g$, in water-plasticized carbohydrates and sugars.[4−9]

Protein hydration properties have been investigated at various temperatures and in frozen aqueous solutions.[10−12] Contrary to vitrification of a water-plasticized carbohydrate phase in cryoprotectant systems,[4] hydration water in protein (metmyoglobin), depending on its quantity, was found using differential scanning calorimetry (DSC) and infrared spectroscopy (IR) to vitrify at 180−270 K.[10] Vitrification of hydration water on the three-dimensional protein structure resulted in $\alpha$-relaxation of the water, as was found by spectroscopic studies.[10] Studies using dielectric spectroscopy have reported multiple relaxations for hydration water, protein, and solvents as well as $\alpha$- and $\beta$-type relaxations of protein hydration water, including a crossover to non-Arrhenius temperature dependence at low temperatures and $\beta$-type relaxations of local water fractions, particularly at hydration levels above 0.300 g of $H_2O$/g of protein.[13−17] On the other hand, vitrification of a protectant carbohydrate on protein surfaces was thought to be a prerequisite, although not sufficient without hydration water replacement through carbohydrate−protein hydrogen bonding

**Received:** February 16, 2015
**Revised:** May 6, 2015





DOI: 10.1021/acs.jpcb.5b01593
J. Phys. Chem. B XXXX, XXX, XXX−XXX

Table 1. BWP−GF Systems

| solids ratio (BWP:GF) | water (%, mass) | water activity ($a_w$) | glass transition (onset $T$, K) | water in BWP (g/g BWP) | water in GF (g/g GF) | water ratio GF/BWP |
|---|---|---|---|---|---|---|
| 45:21 | 12.0 | 0.638 | 222 | 0.102 | 0.210 | 2.059 |
| 45:28 | 14.1 | 0.660 | 216 | 0.115 | 0.244 | 2.122 |
| 45:35 | 15.8 | 0.685 | 214 | 0.134 | 0.256 | 1.910 |
| 45:42 | 17.1 | 0.695 | 211 | 0.142 | 0.276 | 1.944 |
| 45:24 | 18.8 | 0.798 | 206 | 0.188 | 0.314 | 1.670 |
| 45:20 | 23.5 | 0.855 | 197 | 0.269 | 0.396 | 1.472 |
| 45:15 | 29.4 | 0.907 | 189 | 0.391 | 0.492 | 1.259 |
| 45:45[a] | 61.9 | 0.966 | 211[b] | 0.163 | 0.276 | 1.693 |
| 45:22.5[a] | 67.6 | 0.985 | 211[b] | 0.163 | 0.276 | 1.693 |

[a]BWP dissolved to 25.0% (mass) in water before mixing with 80.0% (mass) GF syrup. [b]Maximally freeze-concentrated solids.

for long-term stabilization of the protein conformation.[1] A high correlation of protein stability with $\beta$-relaxation of the carbohydrate glass was also related to protein stability in the vitrified structures.[3] It appears that in aqueous carbohydrate−protein systems, water molecules may hydrate protein structures and also vitrify as hydration water. Proteins as dispersed macromolecular particles in an aqueous system may interact with water molecules quite differently from small carbohydrates and solutes,[16] particularly as water molecules are known to present a high mobility in amorphous carbohydrate glasses.[18] Significant differences in the molecular structures and size of small carbohydrates and proteins and the presence of hydrophobic structures and interactions in proteins[11] support a hypothesis of poor miscibility and molecular segregation of proteins and aqueous carbohydrates in frozen materials. As a result, vitrification of protein hydration water, besides vitrification of the water-plasticized cryoprotectant carbohydrates in a freeze-concentrated carbohydrate-rich phase, may occur in freeze-concentrated protein and carbohydrate−protein systems. Although the hydrogen-bonded network of the protein in aqueous media is underpinning conformational stability,[11] physicochemical changes occurring at low water contents and low temperatures of aqueous protein and carbohydrate−protein systems are poorly understood.

The present study investigated water-content-dependent structural relaxations, mechanical $\alpha$-relaxations, glass transitions, and antiplasticization of the protein hydration water using bovine whey protein (BWP) and an aqueous BWP−glucose−fructose (GF) model typical of aqueous cryoprotectant systems as well as food and pharmaceutical formulations. Individual fractions of unfrozen water for the BWP and GF components were quantified, suggesting separate roles of the hydration water and carbohydrate phase in the frozen state behavior of aqueous protein−carbohydrate (cryoprotectant) systems. The vitrified unfrozen aqueous GF may surround the hydrated BWP, which could be illustrated as a solid protectant surface around the protein hydration interface, and in such a model, the hydrated BWP molecules could exist as segregated particles within the continuous unfrozen GF phase. A corresponding mechanism of protein stabilization is likely to apply in dehydration and anhydrobiosis.

## MATERIALS AND METHODS

**Sample Preparation.** The protein was spray-dried bovine milk whey protein isolate (BWP at 0.050 g of $H_2O$/g of solids and water activity, $a_w$, of 0.310; Isolac, Carbery Food Ingredients, Ballineen, Co. Cork, Ireland). BWP is composed of $\alpha$-lactalbumin ($\alpha$-LA), $\beta$-lactoglobulin ($\beta$-LG), lactoferrin and other immunoglobulins, and bovine serum albumin (BSA) at a natural ratio of 20:55:14:7. The water content of the BWP was determined by dehydration in a vacuum oven at 330 K for 24 h. Purified $\alpha$-LA and $\beta$-LG were obtained from Davisco Foods International, Inc. (Eden Prairie, MN, U.S.A.). D-(+)-Glucose (G; ≥ 99.5% GC), D-(−)-fructose (F; ≥ 99.0%), and salts for preparation of saturated salt solutions were from Sigma-Aldrich, Co. (St. Louise, MO, U.S.A.). Steady-state water contents for the BWP were obtained gravimetrically after equilibration (>40.0 h) in vacuum desiccators over saturated salt solutions of known water vapor pressures at room temperature.[19] GF crystals at 1:1 mass ratio were co-melted by heating and cooling to obtain an anhydrous glass or dissolved in DI water to obtain 70 (mass) and 80% (mass) solutions. A constant quantity of BWP at 0.310$a_w$ was homogeneously blended with various amounts of the 70.0% GF solution to prepare small quantities of the GF−BWP systems (up to 100 g in total) (Table 1). BWP was also prehydrated at a 1:3 mass ratio with deionized (DI) water prior to subsequent adjustment of the GF concentration with the 80.0% GF solution to obtain 1:1 and 2:1 BWP:GF solids mass ratios. DI water was purchased from KB Scientific Ltd. (Cork, Ireland) and used in all experiments. The systems prepared included (i) $\alpha$-LA, $\beta$-LG, and BWP for thermal transitions at 0.761$a_w$ and in excess water at a 1:3 protein:water ratio, (ii) BWP at steady-state water contents corresponding to various $a_w$ values at room temperature (measured at 298 K), and (iii) BWP−GF systems given in Table 1.

**Water in Protein.** *Water Sorption.* Water sorption was determined for the BWP gravimetrically (samples of 1 g in 10 mL glass vials) using triplicate (minimum) samples to establish the full water sorption isotherm, and the Guggenheim−Anderson−de Boer (GAB) model was fitted to water sorption data.[20] Both the Brunauer−Emmett−Teller (BET) and GAB monolayer water contents were calculated using the experimental water sorption data.[20] Noncrystalline solids, such as protein or carbohydrate solids, do not show equilibrium water contents but a nonequilibrium metastable molecular arrangement with $a_w$ defined by the water content and temperature. BWP equilibration over saturated salt solutions (LiCl, 0.114$a_w$; $CH_3COOK$, 0.231$a_w$; $MgCl_2$, 0.332$a_w$; $K_2CO_3$, 0.441$a_w$; $Mg(NO_3)_2$, 0.545$a_w$; $NaNO_2$, 0.656$a_w$; NaCl, 0.761$a_w$; KCl, 0.843$a_w$) in vacuum desiccators provided closed systems where an exact water vapor pressure (confirmed by $a_w$ measurement) of the saturated solution at room temperature was established rapidly.[20] The water vapor pressure in the BWP was controlled to obtain a range of $a_w$ ($a_w = p/p_0$, where, at the same constant temperature, $p$ is the vapor pressure of water in the system and


DOI: 10.1021/acs.jpcb.5b01593
J. Phys. Chem. B XXXX, XXX, XXX−XXX

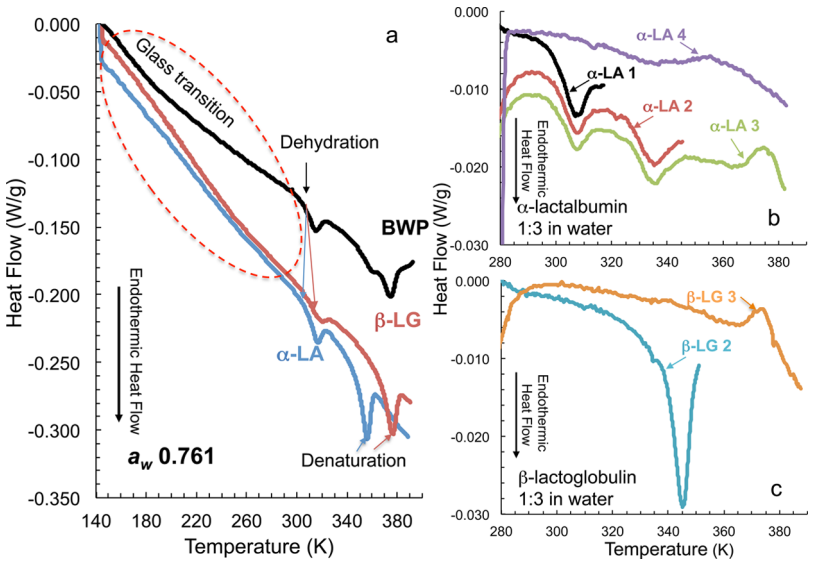


**Figure 1.** DSC thermograms of dehydrated BWP and its main components, $\alpha$-LA and $\beta$-LG at a water activity, $a_w$, of 0.761 measured in heating from 143 to 393 K at 0.083 K $s^{-1}$ (a). At low temperatures, a reversible and broad glass transition occurred over a large temperature range. A reversible but time- and water-content-dependent endotherm (or possibly exotherm) shown as "dehydration" (or "hydration" if exothermic) (a), which indicated a conformational relaxation and variation in the protein hydration level, was followed by endothermic denaturation. (b) Dehydration endotherm ($\alpha$-LA 1) in the first heating to 318 K for a 1:3 $\alpha$-LA solution and in reheating cycles after cooling to 273 at 0.167 K $s^{-1}$. $\alpha$-LA 1 was followed by endothermic denaturation of $\alpha$-LA ($\alpha$-LA 2) in reheating to 346 K. The dehydration and denaturation endotherms were reversible for $\alpha$-LA and reappeared until reheating to 383 at 0.083 K $s^{-1}$ after a second cooling, while an exothermic, irreversible aggregation ($\alpha$-LA 3) occurred in heating to above 365 K. After final cooling and reheating at the same cooling and heating rates, only a continuation of aggregation was shown by a broad exotherm ($\alpha$-LA 4). The 1:3 solution of $\beta$-LG (c) showed no dehydration endotherm, heating to 353 K produced an irreversible denaturation endotherm ($\beta$-LG 2), and after recooling an exothermic aggregation occurred above 365 K ($\beta$-LG 3) during reheating to 383 K. Heating thermograms of subsequent heating−recooling−reheating steps are shown for the same respective samples in (b) and (c).

$p_0$ is the vapor pressure of pure water) to adjust the hydration water content of the BWP. We refer to $a_w$ of the hydration water because water content values exclude information on the thermodynamic distribution of water within materials and global water contents alone cannot be used to quantify the water distribution within a protein or multicomponent system. The $a_w$ at steady state, however, can be assumed to apply across a protein molecule or a complex material, and the corresponding water contents of structural units or fractions of various molecular species such as carbohydrate and protein components can be derived from their individual water sorption data.[20]

*Protein Hydration.* BWP was investigated for its water sorption properties during stepwise temperature heating and cooling over the endothermic transition occurring over the temperature range of 300−330 K (Figure 1). Samples of BWP in duplicate series for at least triplicate $a_w$ readings at each temperature were prepared in $a_w$ measurement cups (AquaLab, Decagon Devices, Pullman, WA, U.S.A.), and each sample was hermetically closed in the AquaLab $a_w$ measurement equipment (AquaLab 4T, Decagon Devices, Pullman, WA, U.S.A.). The sample was equilibrated at 293 K, and $a_w$ was measured. The temperature was ramped at 5.0 K intervals up to 323 K, and $a_w$ was recorded after temperature equilibration at each temperature. A subsequent cooling using 5.0 K ramps with temperature equilibration and $a_w$ monitoring over the same temperature range gave $a_w$ data in cooling.

**Fractional Water Sorption.** The $a_w$ data of the GF−BWP materials were obtained from a minimum of triplicate instrumental measurements (AquaLab 4T, Decagon Devices, Pullman, WA, U.S.A.) at 298 K. At equilibrium and at the same temperature, the $a_w$ across all components of the systems was equal, that is, the steady-state $a_w$ of the GF and BWP components in each GF−BWP system were equal to the $a_w$ measured for the GF−BWP system, and the corresponding fractional water contents of the GF and BWP components could be derived from their individual water sorption isotherms. The water content dependence of the onset $T_g$ of the carbohydrate fraction could be used to obtain water contents in the GF corresponding to the onset $T_g$ measured using DSC. The GAB model using water fractions associated with the GF component was fitted to experimental $a_w$ data for GF−BWP to obtain the water sorption isotherm for the GF fraction. The fractional water content of the BWP in the GF−BWP systems with no ice formation during cooling was given by the difference of the total water content and water associated with the GF fraction (Table 1).

**Differential Scanning Calorimetry.** DSC (Mettler-Toledo, Greifensee, Switzerland) was used to analyze thermal properties and variations in enthalpy of the materials over the range from 133 to 393 K in heating and cooling at 0.033 and 0.833 K $s^{-1}$, respectively. Annealing was used to achieve a maximum freeze concentration of the dissolved solids.[6,8] Transition temperatures were recorded from the onset values determined using the DSC software (STAR$^e$, version 8.10, Mettler Toledo, Schwerzenbach, Switzerland). Hermetically sealed standard 40.0 $\mu$L aluminum pans (Mettler-Toledo, Greifensee, Switzerland) were used with a sample mass of 10.00−15.00 mg in all measurements. The instrument was calibrated for temperature and heat flow over the wide temperature range using the melting point (mp) and heat of melting ($\Delta H_m$) values of *n*-hexane (mp 178 K; $\Delta H_m$ 152 J/g), mercury (mp 234 K; $\Delta H_m$ 11.4 J/g), water (mp 273 K; $\Delta H_m$ 334 J/g), gallium (mp 303 K; $\Delta H_m$ 80.0 J/g), and indium (mp


DOI: 10.1021/acs.jpcb.5b01593
J. Phys. Chem. B XXXX, XXX, XXX−XXX

430 K; $\Delta H_m$ 28.5 J/g). All analyses were carried out in triplicate and using subsequent heating, cooling, and reheating scans to confirm the reversible and irreversible nature of glass and other transitions.

**Dynamic Mechanical Analysis.** Samples (approximately 0.50 g) of BWP with various water contents and $a_w$ (293 K) were prepared in folded stainless steel sheets (Triton Technology Ltd., Lincolnshire, U.K.) and analyzed using a dynamic mechanical analyzer (DMA, Tritec 2000 DMTA, Triton Technology Ltd., Lincolnshire, U.K.) for structural relaxations using the single cantilever bending mode[20] over the temperature range from 123 to 393 K in linear dynamic heating at 0.050 K $s^{-1}$. Data were collected at several frequencies over the range from 0.10 to 10.00 Hz. Relaxation times, $\tau$, at multiple frequencies, $f$, giving $1.60 \times 10^{-2}$ to 1.60 s [$\tau = 1/(2\pi f)$] were derived from loss modulus, $E''$, peak temperatures referred to as $T_\alpha$. Storage modulus, $E'$, data at 0.50 Hz allowed the use of onset temperatures of $\alpha$-relaxations as found from deviation from the linearly decreasing baseline with increasing temperature to confirm the $T_g$ data measured using DSC (Figure 2). A minimum of duplicate samples of each system were analyzed using dynamic measurements and recorded using DMA control software version 1.43.00. The measuring head was connected to a liquid nitrogen tank (1 L; Cryogun, Brymill Cryogenic Systems, Labquip (Ireland) Ltd., Dublin, Ireland) for temperature control. All data are shown as average values measured for a minimum of duplicate samples.

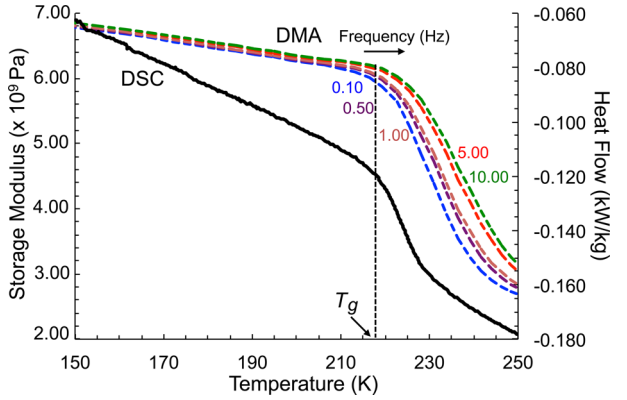


**Figure 2.** Glass transition and $\alpha$-relaxation of GF–BWP solids at a 45:28 BWP:GF ratio and 14.1% (mass) water as measured using DSC and dynamic mechanical analysis (DMA) at various frequencies, respectively. The onset of the glass transition temperature, $T_g$, measured using DSC was in the vicinity of the onset of the decrease in the storage modulus, $E'$, shown for frequencies 0.10, 0.50, 1.00, 5.00, and 10.00 Hz.

## RESULTS AND DISCUSSION

**Bovine Whey Protein.** BWP and its main components, $\alpha$-LA and $\beta$-LG, showed several endothermic and exothermic transitions at $0.761a_w$ during heating from 140 K to temperatures up to 390 K (Figure 1a) and in excess water at 1:3 protein:water, as shown for $\alpha$-LA (Figure 1b) and $\beta$-LG (Figure 1c). The thermal transitions included the weak and broad glass transition of hydration water within the protein,[14,21] an endothermic relaxation[22] assigned as reversible conformational changes corresponding to a molecular relaxation and dehydration ($\alpha$-LA 1), reversible denaturation of $\alpha$-LA[23] assigned as native to molten globule transition of $\alpha$-LA ($\alpha$-LA 2), irreversible denaturation of $\beta$-LG ($\beta$-LG 2), and aggregation, including "gelling" of $\alpha$-LA and $\beta$-LG[24] ($\alpha$-LA 3 and $\beta$-LG 3), which was completed for $\alpha$-LA in a rescan as a broad exotherm ($\alpha$-LA 4). Transitions were also shown in the BWP with the time-dependent appearance of the dehydration endotherm, that is, this endotherm may not be found in an immediate reheating scan but after an annealing treatment or storage.[22] The BWP as well as both $\alpha$-LA and $\beta$-LG at $0.761a_w$ exhibited such dehydration endotherms, while a significant dehydration endotherm at 1:3 protein:water was present only for $\alpha$-LA shown by $\alpha$-LA 1 (Figure 1b).

Hydration of macromolecules may vary depending on temperature and time, as was found when dehydrated proteins were heated to above 310 K to induce an endotherm.[22,25] This endotherm in BWP and its main component proteins was associated with a reversible relaxation affecting protein hydration. Such an endotherm may appear in proteins following storage at normal ambient conditions,[22,25] but in DSC measurements of the BWP, it did not appear in immediate rescanning at all water contents or thermal histories. In the present study, the $\alpha$-LA 1 endotherm was reproduced in the same sample during subsequent heating–cooling cycles within the experimental time scale (Figure 1), but its reappearance in all materials at $0.761a_w$ required rescanning after several days of storage below the transition temperature. In the present study, we equilibrated BWP to various $a_w$ values and monitored the $a_w$ variation during a heating–cooling cycle. DSC studies confirmed the time-dependent nature of the endothermic transition,[22,25] but, as shown in Figure 3, there was also a temperature-dependent $a_w$ hysteresis associated with the transition. At all $a_w$'s, BWP showed an expected increase of $a_w$ with temperature. A low $a_w$ material of $0.114a_w$, however, showed that the $a_w$ during cooling remained higher, which implied a slow relaxation of the BWP components to the original hydration level. Conversely, the hysteresis at the high $a_w$ of 0.843, which exceeded a full hydration of the BWP and ice formation at low temperatures, showed also a higher $a_w$ in cooling. The water content of the BWP at $0.843a_w$ was sufficient to allow a more rapid conformational relaxation, which produced a more pronounced endotherm in the DSC

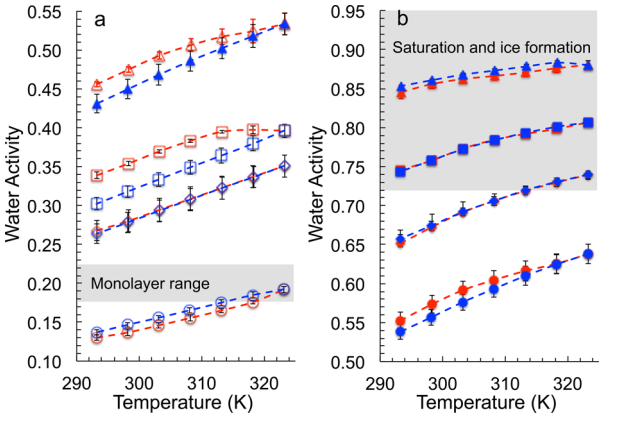


**Figure 3.** Water activity, $a_w$, of BWP equilibrated to various $a_w$'s at room temperature. Samples were hermetically closed for $a_w$ measurements at 5.0 K intervals in a heating–cooling cycle of 293–323–293 K. The monolayer $a_w$ range of BWP (BET, 0.178 g of $H_2O$/g of BWP; GAB, 0.221 g of $H_2O$/g of BWP) (a) as well as the $a_w$ range for ice formation at low temperatures (0. $719a_w$, 0.164 g of $H_2O$/g of BWP) (b) are shown by shaded areas.


DOI: 10.1021/acs.jpcb.5b01593
J. Phys. Chem. B XXXX, XXX, XXX–XXX

scan after storage. The $a_w$ data during cooling confirmed the more rapid relaxation but saturation of hydrogen bonding sites and the apparently higher $a_w$ values. The $a_w$ hysteresis data over the intermediate $a_w$ range showed that the monomolecular water content level ($0.178a_w$, 0.055 g of $H_2O$/g of BWP; $0.221a_w$, 0.062 g of $H_2O$/g of BWP for BET and GAB isotherms, respectively) reversed the $a_w$ hysteresis. BWP at $0.310a_w$ showed an exposure of hydrophilic areas during heating resulting in an increase in hydration and a decrease in $a_w$ during immediate cooling. The hysteresis seemed to depend on the water-content-dependent conformational relaxation time. These time- and water-content-dependent relaxation phenomena with endothermic and exothermic transitions and varying time scales require substantial further studies to explain properties of biological materials at low water contents.

Exposure of the BWP to various water vapor pressure conditions gave materials with $a_w$ and a water content that could be used to follow the water content and $a_w$ dependence of structural relaxations. The precise adjustment of the protein−water content and steady-state stabilization to produce materials with a wide range of $a_w$'s for the sorption isotherm proved invaluable. Figure 1a shows DSC data for BWP and its main component proteins at $0.761a_w$. A weak and broad glass transition occurred in the materials, as was also found for BSA by Panagopolou et al.[21] and is known as a typical property of proteins.[14] The glass transition of the hydration water at water contents from 0.047 to 0.234 g of $H_2O$/g of BWP, however, occurred within a very small fraction of the overall sample mass. Heat capacity changes in such small fractions of a material are included in the overall heat flow and appear over a broad temperature range in DSC measurements. Analysis of such DSC data needs to be supported by complementary measurements of structural relaxations, which may also be difficult to interpret, as shown by dielectric spectroscopy studies.[13−16] Water distribution across the $\alpha$-LA, $\beta$-LG, and other BWP components, such as lactoferrin, could also result in local variation in hydration and antiplasticization of the hydration water by the protein molecules, thus broadening and weakening the glass transition and the temperature range for the change in heat capacity. Therefore, DSC measurements for the detection of such broad glass transitions occurring in a small fraction of protein hydration water may not provide sufficient sensitivity, while dielectric spectroscopic studies have not directly confirmed the nature of relaxations occurring in proteins and hydration water.[16]

The water sorption data with the GAB model isotherm for the BWP are shown in Figure 4. The use of the GAB isotherm was fundamental for the intrapolation of water contents and quantification of the protein hydration water in the GF−BWP systems of known $a_w$. The data also allowed plotting of structural relaxation times of the DMA measurements against water content and $a_w$ of the BWP (Figure 5). The temperatures at the loss modulus, $E''$, peak, $T_a$, for the $\alpha$-relaxation at various frequencies (Figure 5a) against water content showed a systematic, nonlinear increase for temperature of the glass transition of the hydration water (antiplasticization of hydration water) with increasing BWP content (decreasing water content) and a linear relationship against $a_w$ (Figure 5b, inset). Such an increase was expected as the water content decreased from 0.234 to 0.047 g of water/g of BWP (Figure 5b). Water at $>0.843a_w$ in BWP (0.234 g of $H_2O$/g of BWP) showed ice formation in heating using DSC (Figure 6b). The quantity of water at $0.843a_w$ concurred with that often reported

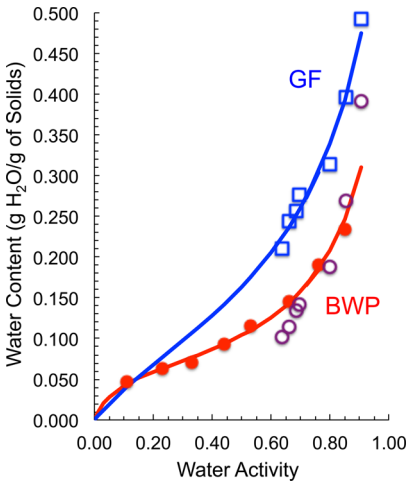


**Figure 4.** Water sorption isotherms for noncrystalline GF (1:1) and BWP at 298 K. The open symbols show fractional water contents derived from measured glass transition data using the Gordon−Taylor (G−T) model for the GF solids with measured water activity, $a_w$, for the GF−BWP systems. The BWP isotherm shows the fractional water content in the GF−BWP systems against experimental $a_w$ (open symbols) and the experimental water contents from the gravimetric study at various $a_w$ conditions (closed symbols). The solid lines show the GAB fit to glass-transition-derived water content data of GF and to gravimetric water sorption data of BWP.

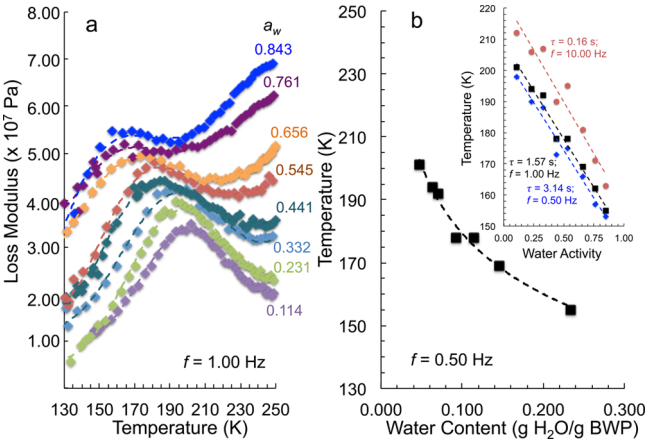


**Figure 5.** DMA data showing the loss modulus, $E''$, of BWP at water activities, $a_w$, of 0.114−0.843 at a 1.00 Hz frequency, $f$, (a) and the temperature at the $E''$ peak, $T_\alpha$, against the water content at $f$ = 0.50 Hz with corresponding relaxation time $t$ = 3.14 s (b). The linear relationship of $T_\alpha$ at $f$ = 0.50, 1.00, and 10.00 Hz against $a_w$ (293 K) is shown in the inset diagram (b). The dynamic heating rate was 0.050 K $s^{-1}$.

as the protein hydration water content, that is, 0.200−0.300 g of water/g of protein that remains unfrozen in aqueous systems.[12] Such unfrozen water, possibly as a solid noncrystalline material within the protein molecules at low temperatures,[12] was hydrogen bonded to the protein[16,21] but was shown by structural relaxation data (Figure 5a) to undergo a glass transition at temperatures above the $T_g$ of pure, noncrystalline water of 136 K.[26,27]

Studies of $\alpha$- and $\beta$-relaxations of water in aqueous systems seldom report systematic structural relaxation data, as shown for BWP in Figure 5a, for anhydrous and low water systems.[16] Panagopoulou et al.[21] illustrated that water in BSA−water systems at low $a_w$ was located at primary sorption sites and as


DOI: 10.1021/acs.jpcb.5b01593
J. Phys. Chem. B XXXX, XXX, XXX−XXX

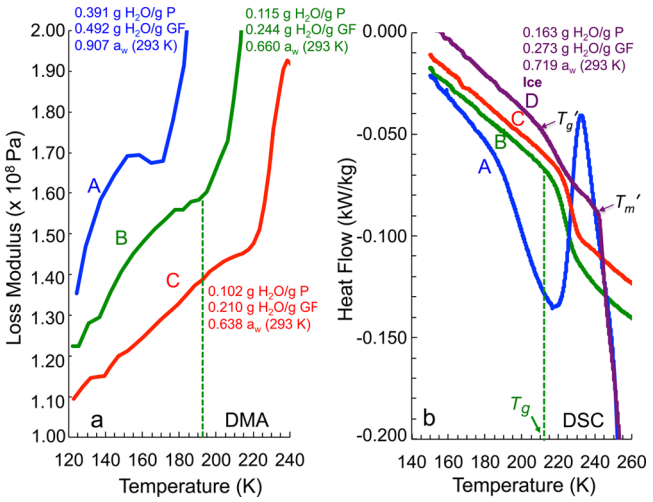


**Figure 6.** Loss modulus, $E''$, data showing structural relaxations for aqueous BWP and GF fractions in GF–BWP solids at various GF:BWP ratios and water contents in heating using DMA at 0.050 K $s^{-1}$ and 1.00 Hz (a) and glass transition and ice melting measured in heating using DSC at 0.083 K $s^{-1}$ (b). BWP:GF ratios in solids were 3:1 (A), 9:8 (B), 3:2 (C), and 2:1 (D). DSC data showed a low-temperature glass transition and ice formation during heating with a corresponding devitrification exotherm (A) and a maximum freeze concentration as a result of annealing at a temperature below the onset of ice melting at 239 K with the initial water-content-independent glass transition temperature, $T_g'$ (211 K), and ice melting temperature, $T_m'$ (239 K), taken from the onset of the DSC transitions (D). Maximum freeze concentration dispersed ice within the unfrozen, continuous carbohydrate phase where proteins segregated as hydrated particles and showed an uncoupled $\alpha$-relaxation for the aqueous hydration interface (curves A, B, and C in (a)).

clusters in hydrophilic areas. Our data for BWP are in strong agreement with those of Panagopolou et al.,[21] and both the increase in the glass transition of hydration water and its unfrozen nature showed that the strength of hydrogen bonding of water on the BWP increased at $a_w$ below 0.843, corresponding to hydration below 0.234 g of $H_2O$/g of BWP. Structural relaxation phenomena of the BWP at low water contents confirmed an individual, highly water-content-dependent aqueous relaxation corresponding to an uncoupled hydration-water-specific $\alpha$-relaxation (Figure 5a). This finding, despite low activation energy for an $\alpha$-relaxation (approximately 60.0 kJ/mol with some variation with water content), reflecting broadness of the transition, was supported by the frequency dependence of the relaxation, its magnitude corresponding to the mass fraction of the unfrozen water and the water content and $a_w$ dependence of the $\alpha$-relaxation temperature range. The present data also showed that hydrogen-bonding sites in BWP molecules must stiffen in its anhydrous state within the temperature range of 200–250 K as a result of complete dehydration. This temperature range coincided with possible segregation of interfacial water, as was suggested by dielectric spectroscopy and NMR observations.[16,17] Hydration water in protein cavities and surface pores together with strong hydrogen bonding reduces the chemical potential and explains the unavailability of hydration water for freezing. The $T_\alpha$ at each frequency decreased linearly with increasing hydration $a_w$, which implied a molar relationship and possible dependence on the number of water molecules involved in protein–water hydrogen bonding (Figure 5b). The linear decrease of $T_\alpha$ was accounted for the reduced number of available hydrogen-bonding sites at the hydrophilic regions of the protein for the larger number of water molecules and the consequential decrease of antiplasticization of the hydration water rather than water plasticization of the protein that was reported for BSA.[21]

Panagopolou et al.[21] determined the water sorption isotherm of BSA for their study of dielectric relaxations using mechanically compressed samples, but a set of different samples dehydrated from a 30% BSA solution was used to measure thermal properties and the glass transition of BSA at various water contents. DSC data were interpreted to show a glass transition decreasing with increasing water content to a lower limit with the midpoint $T_g$ at 193 K in systems with crystallizing water. Panagopolou et al.[28] used a similar approach and compressed elastin samples for a DSC, thermally stimulated depolarization current (TSDC) technique and a dielectric relaxation spectroscopy (DRS) study to detect relaxations in elastin–water systems at low water contents. The authors reported three different dielectric relaxations of distinct unfrozen water fractions. A dielectric contribution from the unfrozen water was interpreted as a secondary relaxation of hydrophilic polar groups in the primary and secondary hydration shells of elastin triggered by hydration water and was referred to as $\nu$ relaxation of hydration water. The $\nu$ relaxation was dependent on the protein hydration level and appeared at higher temperatures with decreasing elastin hydration. A homogeneous distribution of water as well as full equilibration of compressed protein samples, however, may not have reached equilibrium as no details of equilibration times were reported. Our DMA results showed that the structural relaxation phenomena of BWP over a wide range of hydration water contents resulted from the glass transition and corresponded to the $\alpha$-relaxation of the hydration water. We do not find indications of separate $\alpha$- and $\beta$-relaxations in protein hydration water with a crossover of 180–225 K as was concluded from NMR and dielectric spectroscopy measurements of water in protein and other systems.[16,17] BWP, however, showed a second structural relaxation in the vicinity of the crossover temperature of 225 K, which, instead of being a water relaxation,[17] we assigned to motions within the hydrated protein at higher $a_w$ and particularly at water contents exceeding 0.164 g of $H_2O$/g of BWP ($0.719a_w$), that is, that of the maximum freeze concentration.

**Amorphous G–F.** The glass transition and water plasticization properties of the fructose and glucose component sugars used in the present study are well-known.[6,8,29] The glass transition data for GF were obtained from DSC measurements for the GF–BWP systems (Figure 6b) and aqueous 20.0, 70.0, and 80.0% (% of mass) solutions and anhydrous GF (1:1) melt, as shown in the inset of Figure 7. These systems were studied to monitor water plasticization of the GF fraction with and without ice formation and to allow comparison of the $T_g$ data of the GF–BWP systems as well as to complement glass transition data of the individual sugars.[6,8] Carbohydrates in water typically form a maximally freeze-concentrated glass with approximately 20.0% (mass) unfrozen water in 80.0% (mass) carbohydrate.[4–9] Such freeze-concentrated structures correspond to 2.5 molecules of water for each monosaccharide unit remaining unfrozen and agree with increased strength of the hydrogen-bonded structure with increased lifetime of intermolecular and intramolecular hydrogen bonding at high carbohydrate concentrations.[30]

The water-content-dependent onset temperatures of the glass transition, $T_g$, are shown in Figure 7. State diagrams for


DOI: 10.1021/acs.jpcb.5b01593
J. Phys. Chem. B XXXX, XXX, XXX–XXX

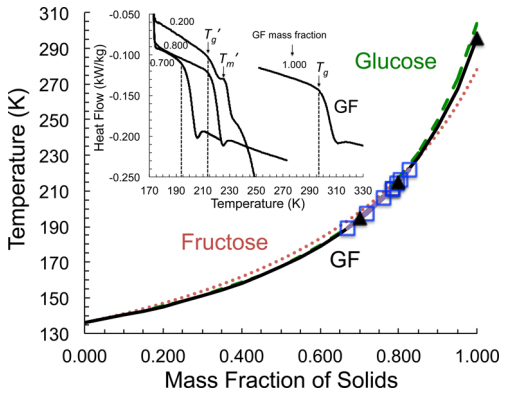


**Figure 7.** G−T fit to the onset glass transition temperature, $T_g$, data of GF (1:1) at various solids contents (closed triangle symbols) shown in the DSC curves of the inset diagram. A maximally freeze-concentrated GF solution with an initial solids fraction of 0.200 was annealed 15.0 min at 223 K, and the onset of the glass transition for the maximally freeze-concentrated GF was measured after cooling to 173 K in heating at 0.083 K $s^{-1}$. The $T_g'$ (215 K) was followed by the onset of ice melting at $T_m'$ (226 K). The $T_g$ data of the GF fractions of the GF−BWP systems (open square symbols) showed water plasticization, and the $T_g$ values concurred the GF data and their G−T fit. The data for noncrystalline fructose and glucose (6,8) are shown for comparison.

fructose and glucose[6,8] showed that in their maximally freeze-concentrated state, the $T_g'$ and $T_m'$ of the individual sugars, referring to the onset temperature of glass transition of the unfrozen carbohydrate−water phase and the onset temperature of dispersed ice melting within the continuous unfrozen carbohydrate−water matrix, respectively, showed little difference.[6] The use of the onset temperatures is necessary as the glass transition may extend to temperatures above the onset of ice melting,[8] and midpoint or endpoint temperatures for the glass transition cannot be experimentally validated.

Data shown in Figure 7 implied that the glass transition values followed the G−T relationship[8,31] with $k$ = 4.10 (eq 1). These data were required to derive water contents associated with the GF fraction of the GF−BWP systems from their respective $T_g$ as the $T_g$ measured for a carbohydrate−protein−water system typically agrees with that of the water-plasticized carbohydrate fraction.[20,32]

**Concentrated Carbohydrate−Protein Systems.** Water fractions associated with the GF component were derived from the calorimetric glass transition onset temperature, $T_g$, data of the GF−BMP systems shown in Figures 3, 5, and 7 and used in the GAB relationship.[20] The $T_g$ values of the GF and GF−BWP were highly water-content-dependent, and the measured $T_g$ values against water content followed the G−T relationship (eq 1; Figure 7), as described for carbohydrate glass formers.[8,20] The fractional water content of the BWP for systems with no ice formation during cooling was given by the difference of the total water content and water associated with the GF fraction (Table 1; Figure 4), as the water distribution according to the $T_g$ and earlier studies could be assumed to occur according to the fractional water sorption properties of the GF and BWP components.[20]

$$T_g = \frac{w_1 T_{g1} + k w_2 T_{g2}}{w_1 + k w_2} \quad (1)$$

A plot of the fractional water contents of the GF and BWP components against $a_w$ with the GAB isotherms gave their water sorption isotherms over a wider $a_w$ range (Figure 4). The water sorption isotherms that showed good agreement with the fractional water and $a_w$ obtained for BWP (Table 1) in the GF−BWP systems could be used to derive water contents for the GF and BWP components at various $a_w$'s. The BWP hydration water fraction at each $a_w$ of the GF−BWP systems could therefore be described by the steady-state water sorption value given by the GAB model.

The $T_g$ data of the GF−BWP systems followed closely the $T_g$ of the GF at various water contents (Figure 7) and confirmed that the corresponding main $\alpha$-relaxation (Figure 6a) originated from the GF fraction plasticized by unfrozen water. Therefore, the measured $T_g$ gave a precise level of water plasticization, and the unfrozen water of the GF component could be quantified. Ice formation took place in the higher water materials, and their maximally freeze-concentrated state could be obtained by annealing. As the total water contents were known for the unfrozen GF−BWP systems, the G−T relationship with the $T_g$ data for the GF gave water fractions associated with the GF, and the quantity of water associated with the BWP (hydration water) could be derived from the difference to the total water content. The GF plasticized by the unfrozen water in the maximally freeze-concentrated state gave by DSC an onset $T_g'$ depressed from 215 K for GF alone[8] to 211 K for GF−BWP (Figure 6b), as measured for annealed (15 min, 238 K) GF−BWP (1:2 of solids) at 68.0% (mass) water content. The maximally freeze-concentrated state had an initial water-content-independent $T_g'$ corresponding to a well-defined unfrozen water concentration plasticizing the GF.[4−9,33] An assumption of an equal $a_w$ of the unfrozen water of the GF fraction and protein hydration water at any temperature to satisfy their thermodynamic balance justified the use of the sorption isotherms to derive water contents of both the GF and BWP components. The BWP hydration water in the maximally freeze-concentrated GF−BWP system showed a quantity that became independent of the initial water content and the carbohydrate content,[4−9,33] that is, maximally freeze-concentrated GF was plasticized by a measurable unfrozen water fraction while the surrounding BWP was maximally freeze-concentrated with a corresponding unfrozen water fraction of the same $a_w$. The unfrozen water fractions in the maximally freeze-concentrated GF−BWP were 0.273 g of $H_2O$/g of GF and 0.164 g of $H_2O$/g of BWP at 0.719$a_w$ (293 K), as shown in Figure 6b. Our method for the experimental quantification of the BWP hydration water in the present study with the corresponding GF water fraction provides a universal method for cryoprotectant systems as well as food and pharmaceutical (biological) materials at various $a_w$'s and at maximum freeze concentration to determine quantitatively (i) protein hydration water in unfrozen and low $a_w$ (dehydrated) as well as maximally freeze-concentrated systems and (ii) the corresponding or unfrozen water in the carbohydrate phase. Such data are extremely important for the understanding and uses of carbohydrate protectants for proteins and biological materials in various processes, including freezing, lyophilization, and dehydration, and to control the stability of the resultant materials.

Structural relaxations for GF−BWP systems at various compositions are shown in Figure 6 with DSC thermograms. The DMA and DSC data showed that vitrification of the BWP hydration water occurred below the GF glass transition as the corresponding $\alpha$-relaxation occurred at lower temperatures. The $E''$ data showed a separate, uncoupled $\alpha$-relaxation of the


DOI: 10.1021/acs.jpcb.5b01593
J. Phys. Chem. B XXXX, XXX, XXX−XXX

BWP hydration water (Figure 6a), while the main $\alpha$-relaxation was segregated (Figure 6a) and corresponded to the DSC glass transition of the GF−unfrozen water (Figure 6b). The onset temperature of the $E''$ peak of the GF agreed with the glass transition onset, $T_g$, measured by DSC.

The data showing separate $\alpha$-relaxations and glass transitions for the GF and BWP fractions disprove the water replacement as well as the $\beta$-relaxation theories presented to explain protein stabilization in carbohydrate materials.[1−3] It appeared that carbohydrate molecules may not hydrogen bond directly on hydrated protein in aqueous carbohydrate−protein systems. Moreover, protein hydration by a quantity of unfrozen water would not be likely if hydration water were directly replaced by carbohydrate molecules. The $\alpha$-relaxation and glass transition data of the GF−BWP system implied that instead of a direct replacement of water by GF on BWP molecules, the BWP hydration water formed an aqueous interface between the protein and the carbohydrate. This interfacial water[21] (hydration shell) was vitrified independently of the bulk aqueous phase and showed antiplasticization by both the BWP and the GF as being sandwiched between the BWP molecules and the continuous GF phase. Our data showed that BWP hydration water vitrified at temperatures below the uncoupled vitrification process of the GF. In general and depending on the carbohydrate, the vitrification of the hydration water and the aqueous carbohydrate phase in biological materials and cryoprotectant systems may occur at different temperatures with consequential individual effects on protein stabilization.

The separate $\alpha$-relaxation of the protein hydration water and that of the bulk GF revealed that hydration water molecules were primarily hydrogen bonded to the BWP and the hydration water provided a bridge for hydrogen bonding of the BWP to the continuous GF phase. The maximally freeze-concentrated state of sugars corresponds to 7−8 hydrogen bonds between each hexose unit and water molecules.[34] The GF−BWP showed 2.75 mol of $H_2O$/mol of GF, implying an increase in hydrogen bonding toward the protein hydration interface. The carbohydrate−water hydrogen bonds are more stable than water−water hydrogen bonds,[30] which explains vitrification of the unfrozen phase rather than ice formation. We conclude that BWP in excess water existed as macromolecular particles or molecular assemblies, which in a maximally freeze-concentrated system segregated into a separate phase from the crystallizing solvent and the unfrozen, continuous GF phase. Despite phase segregation, hydration water may exhibit a high mobility[35] and migration between the protein and the carbohydrate molecules in mixed systems. Hydration water at temperatures above its glass transition may enhance flexibility of the protein. We propose that the stability of a protein in freezing increases below the $T_g'$ of the carbohydrate, but vitrification of the hydration water may increase the mechanical fragility of the protein. The GF−BWP showed vitrification of hydration water at approximately 20 K below the $T_g'$ of the GF. Sucrose and trehalose are common carbohydrate protectants with higher $T_g'$ at 227 and 233 K, respectively.[2,8] At low temperatures as well as lyophilization conditions, proteins in aqueous carbohydrate systems become dispersed with unfrozen hydration water within a solid, noncrystalline, but continuous carbohydrate phase. This mechanism may explain the retention of protein conformation in freezing and dehydration by lyophilization to retain a high biological activity of the rehydrated protein. Correspondingly, in dehydration without freezing, the glass formation around a hydrated protein by a protectant carbohydrate can explain the retention of conformational stability.

**Ternary Carbohydrate−Protein−Water State Diagram.** An aqueous carbohydrate system, such as the GF of the present study, shows a well-established water-content-dependent glass transition that appears in DSC measurements and as an $\alpha$-relaxation in dielectric and mechanical analyses.[4−9] Binary carbohydrate−water state diagrams have proven to be valuable representations of concentration- and temperature-dependent state and phase transitions for various applications, such as freezing and dehydration.[4−9] State diagrams are supplemented phase diagrams that show the binary phase diagram of a water−solute system supplemented with data of amorphous states formed by the water−solute system.[33]

Although a ternary and particularly a frozen or cryopreserved system may have a simple composition of a purified protein, cryoprotectant carbohydrate, and water, the system becomes freeze-concentrated at low temperatures with a resultant complex distribution of ice and unfrozen water within amorphous components. The present study provided for the first time data that could be used to establish a ternary state diagram for a composite aqueous carbohydrate−protein system. The state diagram shows a separate $T_g$ curve for the aqueous carbohydrate, as shown in Figure 8. The water plasticization of the GF component agreed with the G−T relationship fitted to the $T_g$ data of the GF component of the GF−BWP systems (Figures 7 and 8). As the freeze concentration of the GF component occurred during ice formation and was achieved by annealing of GF−BWP systems with a GF mass fraction < $C_g'$ ($C_g'$ is the GF mass fraction of the maximally freeze-concentrated GF component in unfrozen water with unfrozen water mass fraction $W_g' = 1 - C_g'$ corresponding to a glass transition onset at $T_g'$), the $T_g'$ gave a precise measure of the unfrozen water content plasticizing the GF of the GF−BWP systems. The $T_g'$ for the maximally freeze-concentrated GF−BWP systems given in Table 1 as measured using DSC (Figure 6b) was found at 211 K, and $W_g'$ was 0.216 (0.273 g of $H_2O$/g of GF). The $C_g'$ could be used to derive the $a_w$ corresponding to the unfrozen water content of the maximally freeze-concentrated system. The ternary state diagram was established by supplementing the binary GF state diagram with the sorption isotherms of the GF and BWP components. As the $T_g$ curve corresponded to the GF in water at various mass fractions, the corresponding $a_w$ was given by the sorption isotherm of GF. The assumption of equilibrium of $a_w$ for the GF and BWP components in GF−BWP systems justified determination of the BWP hydration water contents using the GF $a_w$ data at various water contents to obtain the BWP hydration water content from the BWP sorption isotherm at the same $a_w$ (Figure 8). Inclusion of the GF and BWP isotherms in the binary state diagram of GF was necessary to supplement the binary state diagram to provide universal data for the water distribution across the GF−BWP components in ternary systems.

In the present study, we showed that the BWP hydration water vitrified at low temperatures, and BWP hydration water gave an $\alpha$-relaxation in the GF−BWP systems. The $T_\alpha$ at 0.50 Hz of the BWP hydration water occurred at lower temperatures than the $T_\alpha$ measured for the BWP in the GF−BWP systems, as shown in Figure 8. The increased $T_\alpha$ of the GF−BWP and the difference to that of the BWP alone were accounted for in the additional antiplasticization of the hydration water by the GF phase. These data were included in the ternary state diagram to


DOI: 10.1021/acs.jpcb.5b01593
J. Phys. Chem. B XXXX, XXX, XXX−XXX

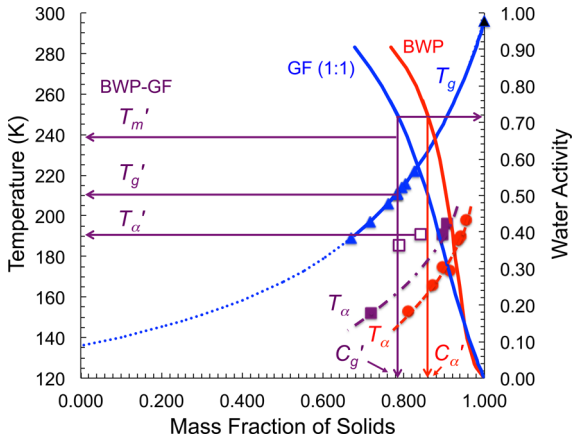


**Figure 8.** State diagram for ternary, aqueous BWP and GF solids systems. The experimental glass transition temperature, $T_g$ (DSC onset), data are shown with the G−T relationship ($k$ = 4.10) prediction for the unfrozen GF (1:1) (blue line and triangle symbols) fraction of the BWP−GF systems. The experimental glass transition temperature of the maximally freeze-concentrated GF fraction, $T_g'$, at 211 K with the onset of ice melting temperature, $T_m'$, at 239 K gave the corresponding unfrozen water content of the GF fraction (unfrozen water mass fraction, $W_g' = 1 - C_g' = 0.216$ or 0.273 g of $H_2O$/g of GF). The GF and BWP mass fractions and corresponding water activity, $a_w$, values are shown by the GAB sorption isotherms fitted to experimental data for BWP (red) and GF (blue). The $a_w$ of the maximally freeze-concentrated solids composition was given by the GF sorption isotherm measured at 293 K as the corresponding water content was constant and temperature-independent. The assumption of an equal $a_w$ of BWP and GF at 293 K was used to derive the mass fraction of the BWP hydration water from the BWP water sorption isotherm. The experimental DMA loss modulus, $E''$, and peak temperatures, $T_\alpha$, at 0.50 Hz measured for the BWP hydration water (red round symbols) and BWP hydration water of the BWP−GF systems (violet square symbols) with additional antiplasticization caused by the GF (increased $T_\alpha$ of the BWP hydration water in the BWP−GF systems) are shown at various mass fractions of BWP solids. Systems with BWP−GF ratios of 45:20 and 45:24 are shown by open squares to indicate their water distribution ratio being close to that of the maximally freeze-concentrated system (Table 1). The $T_\alpha'$ of the BWP hydration water in BWP−GF systems at a maximum freeze concentration (191 K) corresponded to the BWP hydration water mass fraction ($W_g' = 1 - C_g' = 0.140$ or 0.163 g of $H_2O$/g of BWP), as was given by the BWP sorption isotherm.

emphasize the water distribution across the GF and BWP components and the separate vitrification of the hydration water fraction of the BWP component in GF−BWP at low temperatures (Figure 8). It also appeared that BWP hydration water in the maximally freeze-concentrated GF−BWP systems vitrified in a separate glass transition, which corresponded to the $T_\alpha'$ of 191 K at 0.50 Hz (Figure 8). The quantity of hydration water in the BWP could be derived from the $a_w$ of the GF fraction as the collective $a_w$ of the components with their individual water contents was equal at equilibrium. The maximally freeze-concentrated system had $0.719a_w$, and the corresponding equilibrium water contents (unfrozen water fraction, $W_g'$) for the unfrozen GF and BWP components were 0.273 g of $H_2O$/g of GF ($W_g' = 0.216$) and 0.163 g of $H_2O$/g of BWP ($W_g' = 0.140$), respectively (Figures 6 and 8). Furthermore, the ternary state diagram showed the BWP hydration water contents in GF−BWP systems at various $a_w$'s and total water contents as they could be derived from the BWP sorption isotherm. The solids composition and water distribution ratio within the GF−BWP components (Table 1) explained variations of $\alpha$-relaxation temperatures of the interfacial water as systems with similar water distribution ratios to that of maximally freeze-concentrated systems showed $T_\alpha$ in the vicinity of $T_\alpha'$ at 0.50 Hz (Figure 8).

State diagrams such as that of the GF−BWP system can be used in future studies of carbohydrate−protein systems to evaluate effects of protein hydration and vitrification phenomena on cryoprotection and protein stability. As most biological materials contain carbohydrates and proteins in mixed systems, the present study has shown that the information on vitrifcation properties of one component, such as a protectant carbohydrate only, may not be sufficient for the understanding of the complex nature of state and phase behavior of aqueous multicomponent and multiphase systems.

## AUTHOR INFORMATION

### Corresponding Author

*Phone: +353-21-490 2386. E-mail: yrjo.roos@ucc.ie.

### Author Contributions

This manuscript was written through contributions of all authors. All authors have equal contributions and have given approval to the final version of the manuscript.

### Funding

This research was funded by the Irish Department of Agriculture, Food and Marine, Project 11-F-001.

### Notes

The authors declare no competing financial interest.

## REFERENCES

(1) Crowe, J. H.; Carpenter, J. F.; Crowe, L. M. The Role of Vitrification in Anhydobiosis. *Annu. Rev. Physiol.* **1998**, *60*, 73−103.
(2) Kilburn, D.; Townrow, S.; Meunier, V.; Richardson, R.; Alam, A.; Ubbink, J. Organization and Mobility of Water in Amorphous and Crystalline Trehalose. *Nat. Mater.* **2006**, *5*, 632−635.
(3) Cicerone, M. T.; Douglas, J. F. $\beta$-Relaxation Governs Protein Stability in Sugar−Glass Matrices. *Soft Matter* **2012**, *8*, 2983−2991.
(4) Levine, H.; Slade, L. A Polymer Physico-chemical Approach to the Study of Commercial Starch Hydrolysis Products (SHPs). *Carbohydr. Polym.* **1986**, *6*, 213−244.
(5) Levine, H.; Slade, L. Thermomechanical Properties of Small-Carbohydrate−Water Glasses and 'Rubbers'. *J. Chem. Soc., Faraday Trans. 1* **1988**, *84*, 2619−2633.
(6) Roos, Y.; Karel, M. Nonequilibrium Ice Formation in Carbohydrate Solutions. *Cryo-Letters* **1991**, *12*, 367−376.
(7) Roos, Y. H. Glass Transition Temperature and Its Relevance in Food Processing. *Annu. Rev. Food Sci. Technol.* **2010**, *1*, 469−496.
(8) Roos, Y. Melting and Glass Transitions of Low Molecular Weight Carbohydrates. *Carbohydr. Res.* **1993**, *238*, 39−48.
(9) Buera, M. P.; Roos, Y.; Levine, H.; Slade, L.; Corti, H. R.; Reid, D. S.; Auffret, T.; Angell, C. A. State Diagrams for Improving Processing and Storage of Foods, Biological Materials and Pharmaceuticals. *Pure Appl. Chem.* **2011**, *83*, 1567−1617.
(10) Doster, W.; Bachleitner, A.; Dunau, R.; Hiebl, M.; Lüscher, E. Thermal Properties of Water in Myoglobin Crystals and Solutions at Subzero Temperatures. *Biophys. J.* **1986**, *50*, 213−219.
(11) Halle, B. Protein Hydration Dynamics in Solution: A Critical Survey. *Philos. Trans. R. Soc. London, Ser. B* **2004**, *359*, 1207−1224.
(12) Doster, W. The Protein−Solvent Glass Transition. *Biochim. Biophys. Acta* **2010**, *1804*, 3−14.
(13) Gainaru, C.; Fillmer, A.; Böhmer, R. Dielectric Response of Deeply Supercooled Hydration Water in the Connective Tissue Proteins Collagen and Elastin. *J. Phys. Chem. B Lett.* **2009**, *113*, 12628−12631.


DOI: 10.1021/acs.jpcb.5b01593
J. Phys. Chem. B XXXX, XXX, XXX−XXX

(14) Jansson, H.; Bergman, R.; Swenson, J. Role of Solvent for the Dynamics and the Glass Transition in Proteins. *J. Phys. Chem. B* **2011**, *115*, 4099−4109.
(15) Mazza, M. G.; Stokely, K.; Pagnotta, S. E.; Bruni, F.; Stanley, H. E.; Franzese, G. More than One Dynamic Crossover in Protein Hydration Water. *Proc. Natl. Acad. Sci. U.S.A.* **2011**, *50*, 19873−19878.
(16) Swenson, J.; Cerveny, S. Dynamics of Deeply Supercooled Interfacial Water. *J. Phys.: Condens. Matter* **2015**, *27*, 033102.
(17) Sattig, M.; Vogel, M. Dynamic Crossovers and Stepwise Solidification of Confined Water: A $^{2}$H NMR Study. *J. Phys. Chem. Lett.* **2014**, *5*, 174−178.
(18) Hills, B. P.; Wang, Y. L.; Tang, H.-R. Molecular Dynamics in Concentrated Sugar Solutions and Glasses: An NMR Field Cycling Study. *Mol. Phys.* **2001**, *99*, 1679−1687.
(19) Greenspan, L. Humidity Fixed Points of Binary Saturated Aqueous Solutions. *J. Res. Natl. Bur. Stand., Sect. A* **1977**, *81A*, 89−96.
(20) Potes, N.; Kerry, J. P.; Roos, Y. H. Additivity of Water Sorption, $\alpha$-Relaxations and Crystallization Inhibition in Lactose−Maltodextrin Systems. *Carbohydr. Polym.* **2013**, *89*, 1050−1059.
(21) Panagopoulou, A.; Kyritsis, A.; Sabater i Serra, R.; Gómez Ribelles, J. L.; Shinyashiki, N.; Pissis, P. Glass Transition and Dynamics in BSA−Water Mixtures over Wide Ranges of Composition Studied by Thermal and Dielectric Techniques. *Biochim. Biophys. Acta* **2011**, *1814*, 1984−1996.
(22) Farahnaky, A.; Badii, F.; Farhat, I. A.; Hill, S. E. Enthalpy Relaxation of Bovine Serum Albumin and Implications for Its Storage in the Glassy State. *Biopolymers* **2005**, *78*, 69−77.
(23) McGuffey, M. K.; Epting, K. L.; Kelly, R. M.; Foegeding, E. A. Denaturation and Aggregation of Three $\alpha$-Lactalbumin Preparations at Neutral pH. *J. Agric. Food Chem.* **2005**, *53*, 3182−3190.
(24) Fitzsimons, S. M.; Mulvihill, D. M.; Morris, E. R. Denaturation and Aggregation Processes in Thermal Gelation of Whey Proteins Resolved by Differential Scanning Calorimetry. *Food Hydrocolloids* **2007**, *21*, 638−644.
(25) Potes, N. Physico-chemical Properties and Component Interactions in High Solids Food Systems. PhD Thesis, University College Cork, Ireland, 2014; https://cora.ucc.ie/handle/10468/1495.
(26) Angell, C. A. Insights into Phases of Liquid Water from Study of Its Unusual Glass-Forming Properties. *Science* **2008**, *319*, 582−587.
(27) Angell, C. A. Supercooled Water: Two Phases? *Nat. Mater.* **2014**, *13*, 673−675.
(28) Panagopoulou, A.; Kyritsis, A.; Vodina, M.; Pissis, P. Dynamics of Uncrystallized Water and Protein in Hydrated Elastin Studied by Thermal and Dielectric Techniques. *Biochim. Biophys. Acta* **2013**, *1834*, 977−988.
(29) Parks, G. S.; Huffman, H. M.; Cattoir, F. R. Studies on Glass II. The Transition between the Glassy and Liquid States in the Case of Glucose. *J. Phys. Chem.* **1928**, *32*, 1366−1379.
(30) Chen, C.; Li, W. Z.; Song, Y. C.; Weng, L. D.; Zhang, N. Hydrogen Bonding Analysis of Hydroxyl Groups in Glucose Aqueous Solutions by a Molecular Dynamics Simulation Study. *Bull. Korean Chem. Soc.* **2012**, *33*, 2238−2246.
(31) Gordon, M.; Taylor, J. S. Ideal Copolymers and the Second-Order Transitions of Synthetic Rubbers. I. Non-crystalline Copolymers. *J. Appl. Chem.* **1952**, *2*, 493−500.
(32) Potes, N.; Kerry, J. P.; Roos, Y. H. Protein Modifications in High Protein−Oil and Protein−Oil−Sugar Systems at Low Water Activity. *Food Biophys.* **2014**, *9*, 49−60.
(33) Corti, H. R.; Angell, C. A.; Auffret, T.; Levine, H.; Buera, M. P.; Reid, D. S.; Roos, Y. H.; Slade, L. Empirical and Theoretical Models of Equilibrium and Non-equilibrium Transition Temperatures of Supplemented Phase Diagrams in Aqueous Systems. *Pure Appl. Chem.* **2010**, *82*, 1065−1097.
(34) Roos, Y.; Karel, M. Amorphous State and Delayed Ice Formation in Sucrose Solutions. *Int. J. Food Sci. Technol.* **1991**, *26*, 553−566.
(35) Lee, S. L.; Debenedetti, P. G.; Errington, J. R. A Computational Study of Hydration, Solution Structure, and Dynamics in Dilute Carbohydrate Solutions. *J. Chem. Phys.* **2005**, *122*, 204511.


DOI: 10.1021/acs.jpcb.5b01593
*J. Phys. Chem. B* XXXX, XXX, XXX−XXX